Beyond Language: Grounding Referring Expressions with Hand Pointing in Egocentric Vision

Ling Li[1], Bowen Liu[2], Zinuo Zhan[3], Pengjie[3], Jiahui Zhong[2], Kenglun Chang[4], and Zhidong Deng[1,*]

[1] Tsinghua University, Beijing, China
liling25@mails.tsinghua.edu.cn
[2] Dalian University of Technology, Dalian, China
[3] Northwestern Polytechnical University, Xi'an, China
[4] Apple, USA
(*) Corresponding Author

Abstract. Traditional Visual Grounding (VG) predominantly relies on textual descriptions to localize objects, a paradigm that inherently struggles with linguistic ambiguity and often ignores non-verbal deictic cues prevalent in real-world interactions. In natural egocentric engagements, hand-pointing combined with speech forms the most intuitive referring mechanism. To bridge this gap, we introduce EgoPoint-Ground, the first large-scale multimodal dataset dedicated to egocentric deictic visual grounding. Comprising over **15k** interactive samples in complex scenes, the dataset provides rich, multi-grained annotations including hand-target bounding box pairs and dense semantic captions. We establish a comprehensive benchmark for hand-pointing referring expression resolution, evaluating a wide spectrum of mainstream Multimodal Large Language Models (MLLMs) and state-of-the-art VG architectures. Furthermore, we propose SV-CoT, a novel baseline framework that reformulates grounding as a structured inference process, synergizing gestural and linguistic cues through a Visual Chain-of-Thought paradigm. Extensive experiments demonstrate that SV-CoT achieves an **11.7%** absolute improvement over existing methods, effectively mitigating semantic ambiguity and advancing the capability of agents to comprehend multimodal physical intents. The dataset and code will be made publicly available.

Keywords: Visual Grounding · Hand-Pointing Grounding · Multimodal Dataset

1 Introduction

Visual Grounding (VG) [4, 17, 24, 74, 106, 108, 116, 120] aims to localize target objects in images based on natural language queries [54, 66, 107], serving as a fundamental capability for natural human-AI interaction [28, 51, 69, 80, 83, 98, 111]. Existing VG methods primarily rely on static third-person perspective images and

Fig. 1: Our dataset features images captured from an egocentric perspective where a hand is pointing towards a target object. The dataset includes four core annotations: Hand Annotation, Target Object Annotation, Image Caption, and Visual QA Pairs. While conventional Referring Expression Comprehension (REC) tasks only support language-assisted localization, our proposed task aims to address referring disambiguation by utilizing physical hand information as opposed to traditional linguistic assistance for target grounding.

purely textual descriptions for object localization [16,20,47,55,68,75,101,113,116]. However, this paradigm faces fundamental challenges in real-world interactive scenarios: language inherently exhibits ambiguity [32,57], while humans heavily depend on non-linguistic cues (e.g., gestures) for referential disambiguation in daily communication [10,27,29,36,37,53,88]. For instance, when a user says "pass me that one" models struggle to identify the intended referent without gestural context. Figure 1 illustrates the significant difference between our proposed method and current approaches on the referring question-answering task [88,109].

In physical interactions, the synergy between hand gestures and language constitutes the most natural and efficient referring mechanism [14,42,73,88]. A typical scenario involves a user wearing AR glasses [12,58,71] pointing at an object and asking "What is this?"—the finger direction directly resolves linguistic ambiguity [23,52] and precisely guides attention [58,102] to the target [23,40,42,86]. Despite the ubiquity of such multimodal referring in human interaction, existing VG research has largely overlooked gestural cues in first-person perspectives [2,18]. Mainstream datasets focus on third-person images with descriptive text, lacking modeling of gesture-language coordination in egocentric interactions [18,20,26,31,48,59,68,86,87]. Accordingly, existing benchmark tasks have not incorporated gestures into evaluation protocols, limiting model applicability in embodied AI [30,109] and human-robot collaboration scenarios [33,45].

To bridge this gap, we introduce EgoPoint-Ground—the first large-scale multimodal dataset for first-person hand-pointing referring tasks. The dataset

comprises over 15,000 high-quality samples captured from natural interactive moments in complex scenes. Each sample is annotated with hand bounding boxes, target object bounding boxes, image captions, object captions, category labels, and referring question-answer pairs, providing fine-grained supervision signals for multimodal referring expression resolution. Based on this dataset, we establish a benchmark for hand-pointing referring expression resolution and conduct systematic evaluations of mainstream Multimodal Large Language Models (MLLMs) [1, 3, 8, 22, 38, 62, 92, 100, 110, 118] and visual grounding models. Experimental results demonstrate that existing methods suffer significant performance degradation when gestural cues are absent, quantitatively validating the critical role of hand gestures in resolving linguistic ambiguity.

Furthermore, we propose a novel baseline framework, SV-CoT, which explicitly synergizes gestural and linguistic cues through a Visual Chain-of-Thought reasoning paradigm. The model iteratively reasons about the spatial relationship between finger direction and candidate objects, effectively mitigating ambiguity introduced by purely linguistic descriptions. Experiments on EgoPoint-Ground show that our method achieves a 11.7% performance improvement over language-only baselines, fully demonstrating the necessity and effectiveness of multimodal fusion in real-world interactive scenarios.

Our main contributions are summarized as follows: **(1) Dataset:** We present EgoPoint-Ground, the first large-scale multimodal dataset for first-person hand-pointing referring, containing 15,000+ samples with multi-dimensional annotations including hand poses, object locations, and referring expressions. **(2) Benchmark:** We establish an evaluation benchmark for hand-pointing referring expression resolution and systematically analyze the limitations of existing state-of-the-art models on this task. **(3) Model:** We design a partial-Reasoning-based Visual Chain-of-Thought (SV-COT) baseline model, which fuses gestural and linguistic information via a Visual Chain-of-Thought mechanism, significantly improving referring localization accuracy. **(4) Open-source:** We release the dataset, benchmark code, and model implementation to advance research in multimodal referring and embodied AI.

(a) Distribution of Top 20 Samples by Count **(b)** Word Cloud of Sample Categories **(c)** Word Cloud of Image Caption

Fig. 2: Statistical overview and distribution analysis of the Ego-Point Ground dataset. The dataset encompasses a broad spectrum of everyday objects, accompanied by semantically rich and lexically diverse textual annotations.

Table 1: Feature comparison of EgoPoint versus representative reference datasets.

Dataset	Lang.	Gest.	Embo.	Ego/Exo	Pose	VQA	Source	No. images
PointAt [87]	✗	✓	✓	Ego	✗	✗	Lab	220
ReferAt [86]	✗	✓	✓	Exo	✗	✗	Lab	242
IPO [89]	✗	✓	✓	Exo	✗	✗	Lab	278
IMHF [90]	✗	✗	✓	Ego	✗	✗	Lab	1,716
RefIt [56]	✓	✗	✗	Exo	✗	✗	CLEF	19,894
YourRefIt [18]	✓	✓	✓	Exo	✗	✗	Crowd-Sourced	497,348
RefCOCO [115]	✓	✗	✗	Exo	✗	✗	MSCOCO	19,994
RefCOCO+ [72]	✓	✗	✗	Exo	✗	✗	MSCOCO	19,992
RefCOCOg [75]	✓	✗	✗	Exo	✗	✗	MSCOCO	26,711
Flickr30k ent. [81]	✓	✗	✗	Exo	✗	✗	Flickr30K	31,783
GuessWhat? [25]	✓	✗	✗	Exo	✗	✗	MSCOCO	66,537
Cops-Ref [19]	✗	✓	✗	Exo	✗	✗	COCO/Flickr	75,299
CLEVR-Ref+ [67]	✗	✗	✗	Exo	✗	✗	CLEVR	99,992
Ours	✓	✓	✓	**Ego**	✓	✓	**Mixed/Hybrid**	**15,338**

Note: Ego: Egocentric; Exo: Exocentric; Lang.: Language; Gest.: Gesture; Pose: Pose annotations; VQA: Visual Question Answering; Embo.: Embodied. *Source* indicates the data origin: Lab (expert capture), public datasets (e.g., MSCOCO, CLEVR), or Crowd-sourced (AMT). Mixed/Hybrid denotes a combined collection methodology.

2 EgoPoint Ground Dataset

The EgoPoint-Ground Dataset represents the first high-fidelity and high-complexity egocentric benchmark designed explicitly for hand referential grounding. It features diverse scenarios critical for egocentric interaction, particularly simulating the challenge of referential Question Answering (QA) [6] within smart-glasses settings [96]. The images are meticulously annotated with precise pixel-level joint labels, encompassing a comprehensive set of visual elements: target object bounding boxes, detailed hand poses information, and corresponding natural language descriptions. Table 1 details the comparison between our dataset and existing reference understanding datasets.

Figure 1 provides an overview of the dataset's structure and content. The following sections detail the composition, creation pipeline, and statistical analysis of the EgoPoint-Ground Dataset. More details are in the Appendix.

2.1 Dataset Analysis

Our dataset comprises 15,338 images spanning 140 object categories and over 20 everyday scenarios, including indoor, outdoor, animal, food, street, and kitchen environments. Each image contains an average of 2.8 candidate objects, with 63.7% of samples featuring ≥ 2 objects of the same category and 42.5% of targets exhibiting moderate or severe occlusion. The dataset includes both positive and negative samples, with 2,171 negative samples (14.15%) that further increase localization difficulty. We adopt a two-stage splitting strategy. First, under the mixed split, all data sources are combined and randomly partitioned into training, validation, and test sets at a $7 : 2 : 1$ ratio. Second, to simulate real-world deployment, we employ a domain-adaptive split: real-world data captured by

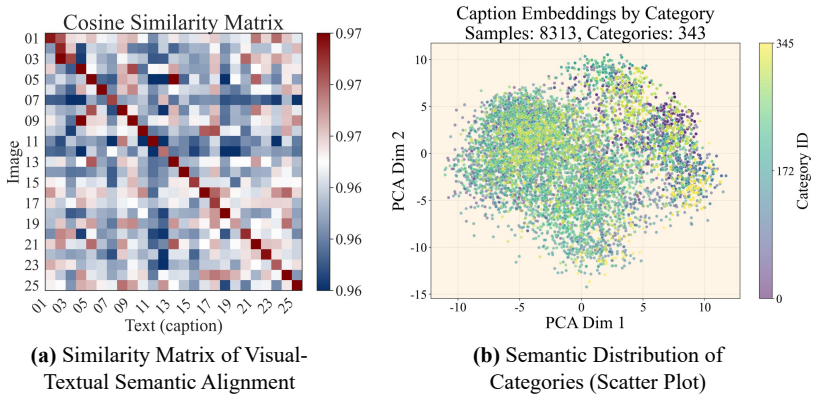

(a) Similarity Matrix of Visual-Textual Semantic Alignment

(b) Semantic Distribution of Categories (Scatter Plot)

Fig. 3: Analysis of Cross-Modal Quality and Semantic Diversity. Figure (a) shows the visual-textual semantic alignment heatmap. The high diagonal similarity confirms strong semantic consistency between images and descriptions. Figure (b) displays the category semantic distribution scatter plot. Image description embeddings are visualized in 2D using PCA (color-coded by category). The points are uniformly distributed without significant clustering, demonstrating the diversity of the dataset's semantic space.

smart glasses is reserved exclusively for testing, while synthetic and generative data are used for training. Specifically, real-captured, synthetically composed, and LLM-generated samples number 6,035, 5,976, and 3,327, accounting for 39.35%, 38.96%, and 21.69% of the dataset, respectively.

Category distribution reveals that person dominates at 47.1%, reflecting the inherent nature of egocentric perception—interactions between the wearer and other individuals constitute the most frequent and fundamental scenario. The remaining 19 major categories are relatively balanced (each ranging from 2.2% to 4.3%), as shown in Figure 2.

Data collection involved 17 participants with diverse demographic attributes (gender, skin tone, age) across varied environments and time periods, ensuring comprehensive representation in both subject and environmental diversity.

Cross-Modal Consistency Analysis We assess the cross-modal consistency between images and captions by randomly sampling N_I images and N_C captions and calculating the cosine similarity between their CLIP-generated [85] visual (v_i) and textual (t_j) embeddings:

$$\text{sim}_{ij} = \frac{v_i \cdot t_j}{|v_i||t_j|}. \tag{1}$$

As illustrated in Figure 3(a), the image-text similarity heatmap exhibits a pronounced diagonal dominance. This robust alignment confirms the precise semantic correspondence of the image-text pairs within our dataset, thereby validating its high annotation quality and consistency.

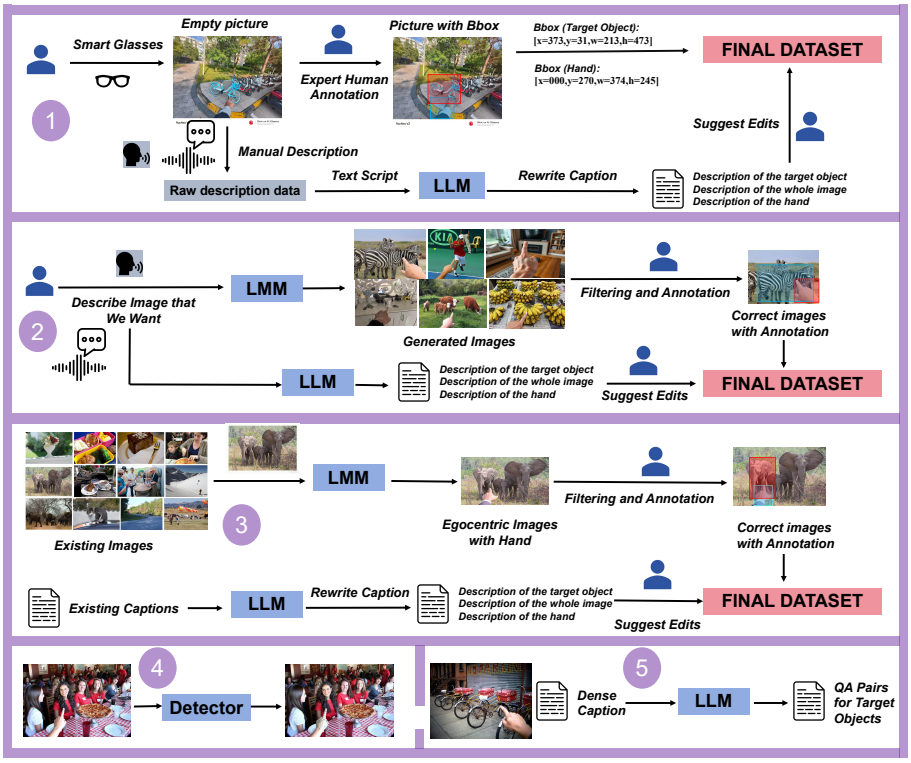

Fig. 4: Overview of the Ego-Point Ground Dataset Collection and Multi-Stage Annotation Pipeline. Stages 1–3 illustrate the raw data acquisition and fundamental annotation workflow. Stage 4 details the extraction of 2D keypoint pose information. Subsequently, Stage 5 focuses on generating high-quality Visual Question-Answering (VQA) pairs for the target objects.

Caption Semantic Diversity Lexical Diversity: Figure 2(c) shows that the dataset emphasizes interactive elements. High-frequency terms include common entities (e.g., "object", "person"), spatial indicators (e.g., "frame", "environment"), and dynamic interaction words (e.g., "pointing", "hand") paired with spatial terms (e.g., "right", "left"). This highlights the dataset's focus on context and dynamic egocentric behaviors.

Semantic Uniformity: To assess semantic diversity, we employ t-SNE [61] to project caption vector representations $t_i \in \mathbb{R}^d$ into a 2D scatter plot, as shown in Figure 3(b). The results demonstrate significant spatial dispersion for most category captions, confirming high semantic diversity. A few categories exhibit tighter clustering, indicating higher linguistic consistency. The dataset's descriptive richness is supported by its broad spatial and categorical diversity.

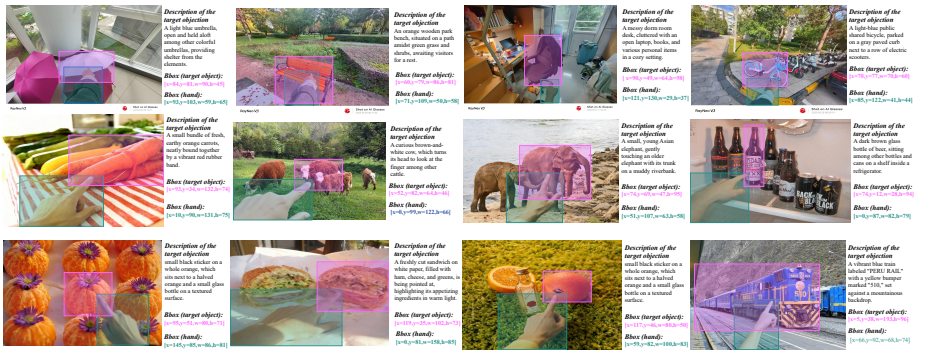

Fig. 5: Image Examples of Ego-Point Ground Dataset. We showcase example images and partial annotations from the dataset, including bounding boxes for the hand and the target object, as well as the corresponding caption for the target object. The first row specifically illustrates data collected from our real-world captures.

2.2 Data Collection Pipeline

The EgoPoint-Ground Dataset uses a Hybrid Data Generation Paradigm to blend real-world diversity with the efficiency of synthetic data, as shown in Figure 4. It combines three main data sources, which are processed and annotated using a dedicated LMM-Aided Synthesis and Editing Pipeline [34, 110]. A partial example of the dataset is shown in Figure 5.

Real-World Data The first source ensures high fidelity by capturing real-world scenarios, We demonstrate this process in Stage 1 of Figure 4. Researchers wearing smart glasses recorded egocentric images of hands pointing at objects in various environments (e.g., schools, supermarkets, homes). Data collectors provided detailed descriptions via voice, which were transcribed and initially drafted by an LLM. Human annotators then reviewed and corrected the LLM-generated text, and manually annotated pixel-accurate bounding boxes for the target object and hand region. This process produced the core caption components: image description, object referent, and hand description.

Synthetic Generation The second component utilizes LMMs for directed image synthesis to efficiently generate challenging referential scenarios that are difficult to capture in the real world, such as complex occlusions or specific lighting conditions. The data collection procedure for this section is shown in Stage 2 of Figure 4. Researchers manually filtered the synthetic Egocentric images to remove unqualified samples. For captioning, participants provided voice descriptions, which were transcribed by an LLM and then subjected to rigorous human review and correction. Target bboxes were manually labeled for precise localization.

Image Editing To efficiently scale the dataset and facilitate domain migration, we employed LMM-aided image editing, as shown in Figure 4, stage 3. We selected

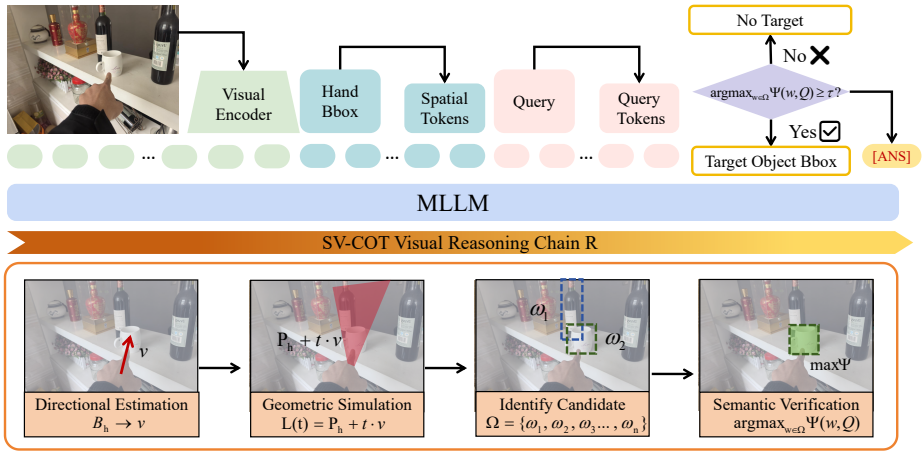

Fig. 6: Architectural overview of the SV-CoT framework. The egocentric hand bounding box $\mathcal{B}^{2D}_{hand}$ is aligned into discrete spatial anchors $\mathcal{T}_{pos}$. Zero-shot grounding is reformulated as a latent reasoning chain $\mathcal{R}$ that sequentially infers: (1) a deictic directional primitive $\boldsymbol{v}$; (2) a virtual ray $\mathcal{L}(t)$ to spatially prune distractors into a candidate set Ω; and (3) a multi-modal semantic verification score Ψ to either resolve the target $BBox_{\mathcal{O}}$ or explicitly reject it via threshold τ.

third-person perspective images from existing datasets [60, 115] and guided a Multi-modal Large Model (LMM) with Egocentric-specific prompts to edit them into egocentric scenes featuring hand pointing. The edited images underwent stringent human screening and secondary annotation to correct LMM-induced pointing inaccuracies. An LLM concurrently structured the captions into three parts: image description, object referent, and hand description.

Auxiliary Annotation and Quality Control To enrich the dataset's dimensions and potential applications, we generated auxiliary annotations (Stage 4 and Stage 5 in Figure 4). An advanced pose estimation model was used to process hand regions in the images, extracting keypoints for Hand Pose annotations, which were refined through human review. Simultaneously, we leveraged the fine-grained captions and an LLM to construct challenging referential QA Pairs.

2.3 Ethical Considerations

The EgoPoint-Ground dataset was collected following strict ethical and privacy guidelines. Participants gave written consent, understanding the data's use and their privacy rights. All images and metadata were de-identified to protect Personally Identifiable Information.

Access is limited to certified researchers through a formal licensing system, with clear usage rules and penalties for violations. We ensure full compliance with ethical standards and prioritize participant privacy.

Table 2: Quantitative results of state-of-the-art models on the D-VQA task, evaluated across both Hybrid (mixed synthetic and captured) and Real-World (naturally captured) datasets. Shaded rows categorize the models into distinct performance tiers, while the Human Study establishes the theoretical upper bound.

Model	**EDG — Hybrid**			**EDG — Real-World**		
	$\mathcal{P}$@0.3 ↑	$\mathcal{P}$@0.5 ↑	$\mathcal{P}$@0.7 ↑	$\mathcal{P}$@0.3 ↑	$\mathcal{P}$@0.5 ↑	$\mathcal{P}$@0.7 ↑
Qwen3-VL-4B [110]	0.743	0.702	0.622	0.747	0.699	0.616
Qwen2.5-VL-3B [100]	0.731	0.671	0.592	0.738	0.632	0.488
Qwen3-VL-8B [110]	0.726	0.676	0.598	0.789	0.701	0.593
Qwen2.5-VL-7B [100]	0.721	0.653	0.563	0.776	0.688	0.533
LLaVA-OneVision-4B [3]	0.679	0.475	0.145	0.654	0.431	0.129
InternVL-3.5-8B [101]	0.554	0.413	0.270	0.592	0.427	0.214
GroundingGPT [59]	0.447	0.358	0.219	0.354	0.259	0.127
DeepSeek-VL2 [103]	0.344	0.293	0.259	0.364	0.296	0.245
LLaVA-v1.5-13B [64]	0.338	0.198	0.079	0.274	0.128	0.042
Ferret-7B [113]	0.282	0.221	0.181	0.258	0.203	0.160
Florence2-Large [105]	0.241	0.188	0.149	0.234	0.193	0.153
Florence2-Base [105]	0.149	0.110	0.080	0.141	0.121	0.075
SV-CoT [Qwen3-vl] (Ours)	**0.795**	**0.756**	**0.718**	**0.820**	**0.818**	**0.727**
Human Study	0.979	0.914	0.846	0.994	0.918	0.874

3 Task Setting

In this section, we establish a comprehensive benchmark for Egocentric Deictic Visual Grounding. By introducing high-quality annotations alongside a robust baseline framework, we provide a solid groundwork to catalyze future research in this novel domain. Leveraging the newly constructed EgoPoint-Ground dataset, we formally define the following evaluation tasks:

3.1 Egocentric Deictic Visual Grounding (EDG)

Motivation: In real-world embodied interactions, deictic gestures and natural language exhibit strong synergistic complementarity. While physical pointing provides an immediate spatial prior, linguistic descriptions supply essential semantic attributes. Because neither modality is independently sufficient to resolve complex spatial or semantic ambiguities, we formulate the Egocentric Deictic Grounding (EDG) task. This benchmark challenges models to seamlessly integrate static hand-pointing cues with linguistic context to achieve robust cross-modal localization.

Task Definition: Formally, the EDG task requires the precise spatial localization of a target object $\mathcal{O}$ through the fusion of visual and linguistic information. The

Table 3: Performance of state-of-the-art models on the D-VQA task across **Hybrid** (mixed synthetic/captured) and **Real-World** (exclusively captured) datasets. The "Human Study" denotes the evaluation results from human participants.

Model	D-VQA (Hybrid)			D-VQA (Real-World)		
	Acc.↑	M-F1↑	Rec.↑	Acc.↑	M-F1↑	Rec.↑
LLaVA-OneVision-8B [3]	0.531	0.519	0.548	0.544	0.525	0.526
LLaVA-OneVision-4B [3]	0.510	0.535	0.547	0.521	0.476	0.487
Qwen3-VL-8B [110]	0.494	0.484	0.490	0.517	0.510	0.503
Qwen3-VL-4B [110]	0.471	0.488	0.495	0.456	0.507	0.489
Qwen2.5-VL-7B [100]	0.457	0.427	0.445	0.444	0.428	0.411
Qwen2.5-VL-3B [100]	0.456	0.461	0.470	0.441	0.527	0.523
DeepSeek-VL2-Small [103]	0.413	0.459	0.455	0.457	0.523	0.506
DeepSeek-VL2 [103]	0.412	0.461	0.473	0.393	0.397	0.390
InternVL-3.5-4B [101]	0.445	0.461	0.445	0.433	0.368	0.367
InternVL-3.5-8B [101]	0.316	0.392	0.381	0.286	0.398	0.380
GroundingGPT [59]	0.334	0.363	0.364	0.392	0.352	0.350
LLaVA-v1.5-13B [64]	0.267	0.249	0.245	0.147	0.150	0.137
Human Study	0.811	0.631	0.653	0.877	0.756	0.753

input consists of an egocentric image $\mathcal{I}$, the 2D bounding box of the pointing hand $\mathcal{B}^{2D}_{hand}$, and an underspecified linguistic referent $\mathcal{D}_{\mathcal{O}}$ (e.g., "this object" or "that boy"). Notably, $\mathcal{D}_{\mathcal{O}}$ identifies the target's category or intent but lacks unique spatial discriminability. Input: $(\mathcal{I}, \mathcal{B}^{2D}_{hand}, \mathcal{D}_{\mathcal{O}})$; Output: The 2D bounding box of the target object, $BBox_{\mathcal{O}}$.

3.2 Deictic Visual Question Answering (D-VQA)

Motivation: The ultimate goal of advanced embodied agents is to achieve meaningful, situated interaction and manipulation. Following successful localization, high-level reasoning about the target object in the environment is often required to determine subsequent actions and intent. The D-VQA task aims to evaluate a model's ability to perform high-level Situated Reasoning on the target object after successfully parsing the hand pointing intent and localization, thereby supporting decision-making and action planning.

Task Definition: Given the image $\mathcal{I}$, the hand's 2D bbox $\mathcal{B}^{2D}_{hand}$, and a specific question about the referred object $\mathcal{Q}$ (eg. "What is this?", "What is the boy wearing? "), the model must provide the answer. Input: $(\mathcal{I}, \mathcal{B}^{2D}_{hand}, \mathcal{Q})$; Output: The answer to the question, $\mathcal{A}$.

3.3 Language-Only Grounding(D-REC)

Motivation: The Language-Only Grounding task follows the paradigm of traditional Referring Expression Comprehension (REC) but is specifically tailored for egocentric deictic scenarios. The motivation is twofold: first, to quantify the model's independent capability to interpret referential linguistic cues (e.g., "this", "this boy") within a first-person visual context; and second, to serve as a rigorous ablation baseline for evaluating the performance gain of multi-modal fusion (as in EDG) over a purely linguistic-driven approach on the same dataset.
Task Definition: Input: $(\mathcal{I}, \mathcal{D}_{\mathcal{O}})$; Output: $BBox_{\mathcal{O}}$.

3.4 Physical Pointing-Only Grounding (POG)

Motivation: This task aims to quantify the independent referencing capability of the hand-pointing pose. By providing only the 2D pose, we evaluate the model's ability to infer spatial pointing intent purely from the static hand configuration. This forms another EDG ablation baseline.
Task Definition: Input: $(\mathcal{I}, \mathcal{B}^{2D}_{hand})$; Output: $BBox_{\mathcal{O}}$.

4 Experiment

4.1 Baseline Method

To bridge the granularity gap between continuous visual coordinates and the discrete linguistic vocabulary of MLLMs, we adopt a coordinate-to-token alignment protocol. Given an egocentric image $\mathcal{I}$ and the referrer's hand bounding box $\mathcal{B}^{2D}_{hand} = [x, y, w, h]$, we apply a spatial quantization function $\phi(\cdot)$ to map each coordinate into N discrete spatial bins (where $N = 1000$):

$$\mathcal{T}_{pos} = \left\{ \langle \text{bin}_c \rangle \mid c \in \mathcal{B}^{2D}_{hand}, \phi(c) = \left\lfloor \frac{c}{L} \cdot (N-1) \right\rfloor \right\} \tag{2}$$

These quantized tokens $\mathcal{T}_{pos}$ serve as **Spatial Anchors**, grounding the LLM's attention to the specific ego-gestural region within the multimodal input stream.

SV-CoT: Spatial-Reasoning-based Visual Chain-of-Thought Instead of treating grounding as a direct regression task, we reformulate it as a structured inference process. We present **SV-CoT**, a zero-shot inference framework instantiated on Qwen3-VL [110]. As depicted in Figure 6, this baseline systematically decomposes the complex deictic intent into a sequential latent reasoning chain $\mathcal{R}$. Formally, the target distribution $P(BBox_{\mathcal{O}} \mid \mathcal{I}, \mathcal{B}^{2D}_{hand}, \mathcal{Q})$ is modeled by marginalizing over a sequence of geometric rationales:

$$P(BBox_{\mathcal{O}} \mid \mathcal{X}_{in}) = \sum_{\mathcal{R}} P(BBox_{\mathcal{O}} \mid \mathcal{R}, \mathcal{X}_{in}) P(\mathcal{R} \mid \mathcal{X}_{in}) \tag{3}$$

where $\mathcal{X}_{in} = (\mathcal{I}, \mathcal{B}^{2D}_{hand}, \mathcal{Q})$ denotes the multimodal input context. The reasoning variable $\mathcal{R} = \{r_{dir}, r_{path}, r_{ref}\}$ is instantiated as a causal chain of linguistic tokens, mimicking human-like spatial deduction:

1. Deictic Intent Parsing (r_{dir}): The model first performs an *anatomical-to-spatial* projection. By analyzing the orientation of the hand within the anchor $\mathcal{B}^{2D}_{hand}$, the MLLM instantiates a directional primitive $\boldsymbol{v} \in \mathbb{R}^2$, effectively transforming local gesture posture into a global pointing prior.

2. Geometric Trajectory Simulation (r_{path}): This primitive defines a virtual ray $\mathcal{L}(t) = \mathcal{P}_{hand} + t \cdot \boldsymbol{v}$, where $\mathcal{P}_{hand}$ denotes the spatial centroid of $\mathcal{B}^{2D}_{hand}$. The model executes a **spatial pruning** operation, identifying a candidate set $\Omega = \{\omega_1, \ldots, \omega_n\}$ of visual regions that satisfy the intersection constraint $\omega_i \cap \mathcal{L}(t) \neq \emptyset$. This effectively filters spatial distractors from cluttered egocentric scenes.

3. Spatio-semantic Verification (r_{ref}): The final phase involves a multi-modal alignment check. The model resolves the target $BBox_{\mathcal{O}}$ by evaluating the semantic consistency Ψ between the linguistic query $\mathcal{Q}$ and the pruned candidates Ω:

$$BBox_{\mathcal{O}} = \begin{cases} \arg\max_{\omega \in \Omega} \Psi(\omega, \mathcal{Q}) & \text{if } \max_{\omega \in \Omega} \Psi(\omega, \mathcal{Q}) \geq \tau \\ \varnothing & \text{otherwise} \end{cases} \tag{4}$$

where τ is a confidence threshold for **explicit rejection**. By parameterizing the zero-shot inference as $\mathcal{Y} = [\mathcal{R}, BBox_{\mathcal{O}}]$, SV-CoT enforces a structural constraint that mitigates spatial hallucination and ensures referential consistency.

4.2 Evaluation Metrics

We evaluate the proposed benchmarks using the following metrics:
Localization Metrics: For EDG, D-REC, and POG tasks, we adopt Precision@τ as the core metric, which measures the proportion of samples where the Intersection over Union (IoU) between the predicted and ground-truth bounding boxes exceeds threshold τ. We report results at $\tau \in \{0.3, 0.5, 0.7\}$ to reflect varying localization precision.
Classification Metrics: For the D-VQA task, we employ Accuracy (Acc.), Macro F1-score, and Macro Recall to assess the correctness of answers. Macro-averaging is specifically used to ensure a fair evaluation across the class-imbalanced distribution of our dataset.

4.3 Experimental Results

Results on Egocentric Deictic Grounding We conduct a comprehensive evaluation of state-of-the-art MLLMs and VG models on the EDG task across both hybrid and real-world scenarios (see Table 2). The results reveal a distinct performance hierarchy: the Qwen3 and Qwen2.5 series lead the field due to their superior vision-language alignment (e.g., Qwen3-VL-8B achieves $\mathcal{P}$@0.5 of 0.701 on real-world), whereas foundational models like Florence2 and LLaVA-v1.5 struggle, with accuracies consistently below 0.34. Notably, while baseline models exhibit a sharp performance decline at higher precision thresholds ($\mathcal{P}$@0.7), highlighting the significant challenge of fine-grained gesture-to-object localization,

Table 4: Performance comparison on conventional REC and dedicated POG tasks. Absolute scores are reported with relative gains/losses compared to the baseline (Inputs are provided without either spatial or linguistic cues) in parentheses.

Model	D-REC			POG		
	$\mathcal{P}$@0.3 ↑	$\mathcal{P}$@0.5 ↑	$\mathcal{P}$@0.7 ↑	$\mathcal{P}$@0.3 ↑	$\mathcal{P}$@0.5 ↑	$\mathcal{P}$@0.7 ↑
Qwen3-VL-4B [110]	0.737 (+0.087)	0.684 (+0.118)	0.605 (+0.123)	0.671 (+0.021)	0.612 (+0.046)	0.532 (+0.050)
Qwen3-VL-8B [110]	0.701 (+0.111)	0.648 (+0.087)	0.561 (+0.077)	0.653 (+0.063)	0.595 (+0.034)	0.514 (+0.030)
Qwen2.5-VL-7B [100]	0.703 (+0.190)	0.638 (+0.160)	0.541 (+0.125)	0.670 (+0.157)	0.611 (+0.143)	0.515 (+0.099)
Qwen2.5-VL-3B [100]	0.665 (+0.169)	0.592 (+0.167)	0.491 (+0.139)	0.575 (+0.079)	0.501 (+0.076)	0.407 (+0.055)
LLaVA-OneVision-4B [3]	0.586 (+0.194)	0.347 (+0.186)	0.088 (+0.071)	0.525 (+0.133)	0.292 (+0.131)	0.065 (+0.048)
LLaVA-OneVision-8B [3]	0.505 (+0.167)	0.258 (+0.110)	0.049 (+0.027)	0.403 (+0.065)	0.181 (+0.033)	0.025 (+0.003)
InternVL-3.5-4B [101]	0.535 (+0.149)	0.402 (+0.135)	0.272 (+0.092)	0.416 (+0.030)	0.305 (+0.038)	0.203 (+0.023)
InternVL-3.5-8B [101]	0.456 (+0.066)	0.325 (+0.045)	0.210 (+0.006)	0.497 (+0.107)	0.311 (+0.031)	0.178 (-0.026)
DeepSeek-VL2-Small [103]	0.443 (-0.001)	0.393 (-0.005)	0.341 (+0.023)	0.375 (-0.069)	0.318 (-0.080)	0.274 (-0.044)
Ferret-7B [113]	0.428 (+0.029)	0.350 (+0.015)	0.261 (-0.001)	0.413 (+0.014)	0.353 (+0.018)	0.281 (+0.019)
GroundingGPT [59]	0.378 (-0.149)	0.261 (-0.169)	0.129 (-0.162)	0.536 (+0.009)	0.443 (+0.013)	0.305 (+0.014)
SV-CoT [Qwen3-vl] (Ours)	**0.814**	**0.750**	**0.694**	**0.694**	**0.639**	**0.556**
Human Study	0.952	0.926	0.819	0.956	0.916	0.806

our method demonstrates remarkable resilience. Specifically, a substantial gap of over 26% persists between the top-performing baseline and the **Human Study** upper bound ($\mathcal{P}$@0.5 $\geq$ 0.914), suggesting that general-purpose MLLMs have yet to master complex "hand-object" spatial logic. Our proposed baseline, **SV-CoT**, explicitly guides spatial reasoning via a Visual Chain-of-Thought, achieving an impressive absolute improvement of 11.7% (0.818 vs. 0.701) in real-world and 5.4% (0.756 vs. 0.702) in hybrid scenarios at $\mathcal{P}$@0.5 over the strongest open-source baselines. Furthermore, SV-CoT effectively maintains a high accuracy of over 0.71 even at the strict $\mathcal{P}$@0.7 threshold, significantly mitigating semantic ambiguity in deictic references. Interestingly, most baseline models perform slightly better in real-world than in hybrid scenarios. This discrepancy arises because the hybrid set

serves as a rigorous stress test, incorporating a higher density of synthetic noise, extreme viewpoint augmentations, and occlusions that surpass the distributional complexity of natural captures.

Results on Deictic Visual Question Answering The D-VQA task requires models to establish deep semantic correlations between hand-pointing gestures and specific linguistic queries within complex visual scenes. As shown in Table 3, LLaVA-OneVision and the Qwen3-VL series demonstrate competitive performance, with LLaVA-OneVision-8B achieving the highest accuracy of 0.544 in real-world scenarios. In contrast, foundational or smaller-scale models (e.g., LLaVA-v1.5) struggle with such gesture-based visual reasoning.

Despite progress by top-tier models, a performance gap of approximately 30% remains relative to the **Human Study** upper bound (Acc. > 0.81). This gap underscores the inherent difficulty for general-purpose MLLMs in precisely mapping spatial coordinates (Hand Bbox) to semantic question-answering, a challenge we define as deictic alignment failure.

Ablation Studies: Linguistic vs. Geometric Cues D-REC and POG evaluate referential understanding using isolated linguistic or physical cues (Table 4). Compared to the multimodal EDG task, all models show significant performance drops, confirming the severe referential ambiguity of unimodal inputs. While Qwen3 maintains a robust $\mathcal{P}@0.5$ of 0.684 in D-REC, POG results expose a critical deficiency in geometric understanding. Models generally perform worse on POG, collapsing at high-precision thresholds (e.g., LLaVA-OneVision-8B drops to 0.025 at $\mathcal{P}@0.7$). This indicates that current MLLMs fail to map the spatial trajectory from "fingertip" to "target" without linguistic aid, revealing a massive gap in physical intent comprehension compared to human performance.

Our baseline, **SV-CoT**, effectively mitigates these restrictions via a Visual Chain-of-Thought. It achieves 0.639 at $\mathcal{P}@0.5$ in POG (an absolute gain of 2.7% over the strongest baseline) and 0.750 in D-REC (a 6.6% gain). This demonstrates that explicit gesture-object spatial modeling effectively overcomes the limitations of isolated geometric or linguistic perception.

5 Conclusion

In this work, we formalized the egocentric deictic visual grounding task, directly addressing the inherent inadequacies of text-only queries in resolving physical interaction ambiguities. Our primary contribution is EgoPoint-Ground, a pioneering large-scale multimodal dataset comprising over 15,000 densely annotated samples that capture hand-gesture and linguistic co-reference. Upon this foundation, we established a rigorous benchmark evaluating a wide spectrum of state-of-the-art MLLMs and visual grounding architectures. Furthermore, we introduced SV-CoT, a robust baseline framework that synergizes gestural primitives and linguistic context through a Visual Chain-of-Thought reasoning mechanism. We will open-source our dataset and models to advance research in embodied AI, egocentric vision, and multimodal interaction.

Limitations and Future Work While EgoPoint-Ground provides a robust baseline, it currently focuses on canonical index-finger pointing in static images, limiting the exploration of complex gestures and continuous spatiotemporal trajectories. Furthermore, extreme cases involving severe occlusion or highly distal targets remain challenging. To capture dynamic pointing intents, future work will expand this paradigm into the video domain.

References

1. Achiam, J., Adler, S., Agarwal, S., Ahmad, L., Akkaya, I., Aleman, F.L., Almeida, D., Altenschmidt, J., Altman, S., Anadkat, S., et al.: GPT-4 Technical Report. ArXiv Preprint ArXiv:2303.08774 (2023)
2. Ahuja, C.: Communication Beyond Words: Grounding Visual Body Motion with Language. Ph.D. thesis, Carnegie Mellon University (2022)
3. An, X., Xie, Y., Yang, K., Zhang, W., Zhao, X., Cheng, Z., Wang, Y., Xu, S., Chen, C., Wu, C., et al.: Llava-onevision-1.5: Fully Open Framework for Democratized Multimodal Training. ArXiv Preprint ArXiv:2509.23661 (2025)
4. Anderson, P., Wu, Q., Teney, D., Bruce, J., Johnson, M., Sünderhauf, N., Reid, I., Gould, S., Van Den Hengel, A.: Vision-and-Language Navigation: Interpreting Visually-Grounded Navigation Instructions in Real Environments. In: Proceedings of the IEEE Conference on Computer Vision and Pattern Recognition. pp. 3674–3683 (2018)
5. Andriluka, M., Pishchulin, L., Gehler, P., Schiele, B.: 2D Human Pose Estimation: New Benchmark and State of the Art Analysis. In: Proceedings of the IEEE Conference on Computer Vision and Pattern Recognition. pp. 3686–3693 (2014)
6. Antol, S., Agrawal, A., Lu, J., Mitchell, M., Batra, D., Zitnick, C.L., Parikh, D.: VQA: Visual Question Answering. In: Proceedings of the IEEE International Conference on Computer Vision. pp. 2425–2433 (2015)
7. Arena, F., Collotta, M., Pau, G., Termine, F.: An Overview of Augmented Reality. Computers **11**, 28 (2022)
8. Bai, J., Bai, S., Chu, Y., Cui, Z., Dang, K., Deng, X., Fan, Y., Ge, W., Han, Y., Huang, F., et al.: Qwen Technical Report. ArXiv Preprint ArXiv:2309.16609 (2023)
9. Bansal, A., Sikka, K., Sharma, G., Chellappa, R., Divakaran, A.: Zero-Shot Object Detection. In: Proceedings of the European Conference on Computer Vision. pp. 384–400 (2018)
10. Bansal, S., Arora, C., Jawahar, C.: My View is the Best View: Procedure Learning from Egocentric Videos. In: Proceedings of the European Conference on Computer Vision. pp. 657–675 (2022)
11. Banyai, A.D., Brișan, C.: Robotics in Physical Rehabilitation: Systematic Review. In: Healthcare. vol. 12, p. 1720 (2024)
12. Bhattacharyya, P., Mitton, J., Page, R., Morgan, O., Menzies, B., Homewood, G., Jacobs, K., Baesso, P., Trickett, D., Mair, C., et al.: Helios: An extremely low power event-based gesture recognition for always-on smart eyewear. In: European Conference on Computer Vision. pp. 168–184. Springer (2024)
13. Carmigniani, J., Furht, B.: Augmented Reality: An Overview. Handbook of augmented reality pp. 3–46 (2011)
14. Chandel, H., Vatta, S.: Occlusion Detection and Handling: A Review. International Journal of Computer Applications **120** (2015)
15. Chen, J., Grubert, J., Kristensson, P.O.: Large Language Model-assisted Speech and Pointing Benefits Multiple 3D Object Selection in Virtual Reality. ArXiv Preprint ArXiv:2410.21091 (2024)
16. Chen, K., Zhang, Z., Zeng, W., Zhang, R., Zhu, F., Zhao, R.: Shikra: Unleashing Multimodal LLM's Referential Dialogue Magic. ArXiv Preprint ArXiv:2306.15195 (2023)
17. Chen, W., Chen, L., Wu, Y.: An Efficient and Effective Transformer Decoder-Based Framework for Multi-Task Visual Grounding. In: European Conference on Computer Vision. pp. 125–141. Springer (2024)

18. Chen, Y., Li, Q., Kong, D., Kei, Y.L., Zhu, S.C., Gao, T., Zhu, Y., Huang, S.: YouRefIt: Embodied Reference Understanding With Language and Gesture. In: Proceedings of the IEEE/CVF International Conference on Computer Vision. pp. 1385–1395 (2021)
19. Chen, Z., Wang, P., Ma, L., Wong, K.Y.K., Wu, Q.: Cops-Ref: A New Dataset and Task on Compositional Referring Expression Comprehension. In: Proceedings of the IEEE/CVF Conference on Computer Vision and Pattern Recognition. pp. 10086–10095 (2020)
20. Cheng, T., Song, L., Ge, Y., Liu, W., Wang, X., Shan, Y.: YOLO-World: Real-Time Open-Vocabulary Object Detection. In: Proceedings of the IEEE/CVF Conference on Computer Vision and Pattern Recognition. pp. 16901–16911 (2024)
21. Chu, Y., Ye, M., Qian, Y.: Fine-Grained Image Recognition Methods and Their Applications in Remote Sensing Images: A Review. IEEE Journal of Selected Topics in Applied Earth Observations and Remote Sensing **17**, 19640–19667 (2024)
22. Chuang, Y.S., Li, Y., Wang, D., Yeh, C.F., Lyu, K., Raghavendra, R., Glass, J., Huang, L., Weston, J., Zettlemoyer, L., et al.: Meta CLIP 2: A Worldwide Scaling Recipe. ArXiv Preprint ArXiv:2507.22062 (2025)
23. Constantin, S., Eyiokur, F.I., Yaman, D., Bärmann, L., Waibel, A.: Interactive Multimodal Robot Dialog Using Pointing Gesture Recognition. In: European conference on computer vision. pp. 640–657. Springer (2022)
24. Dai, M., Yang, L., Xu, Y., Feng, Z., Yang, W.: SimVG: A Simple Framework for Visual Grounding with Decoupled Multi-modal Fusion. In: Proceedings of the Advances in Neural Information Processing Systems. pp. 121670–121698 (2024)
25. De Vries, H., Strub, F., Chandar, S., Pietquin, O., Larochelle, H., Courville, A.: GuessWhat?! Visual Object Discovery Through Multi-Modal Dialogue. In: Proceedings of the IEEE Conference on Computer Vision and Pattern Recognition. pp. 5503–5512 (2017)
26. Deichler, A., O'Regan, J., Beskow, J.: MM-Conv: A Multi-modal Conversational Dataset for Virtual Humans. arXiv preprint arXiv:2410.00253 (2024)
27. Delmas, G., Weinzaepfel, P., Moreno-Noguer, F., Rogez, G.: PoseEmbroider: Towards a 3D, Visual, Semantic-aware Human Pose Representation. In: European Conference on Computer Vision. pp. 55–73. Springer (2024)
28. Duan, J., Yu, S., Tan, H.L., Zhu, H., Tan, C.: A Survey of Embodied AI: From Simulators to Research Tasks. IEEE Transactions on Emerging Topics in Computational Intelligence **6**, 230–244 (2022)
29. Efron, R.: What is Perception? In: Proceedings of the Boston Colloquium for the Philosophy of Science 1966/1968. pp. 137–173 (1969)
30. Fan, Z., Ohkawa, T., Yang, L., Lin, N., Zhou, Z., Zhou, S., Liang, J., Gao, Z., Zhang, X., Zhang, X., et al.: Benchmarks and Challenges in Pose Estimation for Egocentric Hand Interactions with Objects. In: European Conference on Computer Vision. pp. 428–448. Springer (2024)
31. Farkhondeh, A., Tafasca, S., Odobez, J.M.: ChildPlay-Hand: A Dataset of Hand Manipulations in the Wild. In: European Conference on Computer Vision. pp. 101–118. Springer (2024)
32. Fortuny, J., Payrató, L.: Ambiguity in Linguistics. Studia Linguistica **78**(1), 1–7 (2024)
33. Foteinos, K., Angelidis, G., Psiris, A., Argyriou, V., Sarigiannidis, P., Papadopoulos, G.T.: FR-GESTURE: An RGBD Dataset For Gesture-based Human-Robot Interaction In First Responder Operations. arXiv preprint arXiv:2602.17573 (2026)

34. Gao, Y., Gong, L., Guo, Q., Hou, X., Lai, Z., Li, F., Li, L., Lian, X., Liao, C., Liu, L., et al.: Seedream 3.0 Technical Report. ArXiv Preprint ArXiv:2504.11346 (2025)
35. Garcia, E., Jimenez, M.A., De Santos, P.G., Armada, M.: The Evolution of Robotics Research. IEEE Robotics & Automation Magazine **14**, 90–103 (2007)
36. Grauman, K., Westbury, A., Byrne, E., Chavis, Z., Furnari, A., Girdhar, R., Hamburger, J., Jiang, H., Liu, M., Liu, X., et al.: Ego4D: Around the World in 3,000 Hours of Egocentric Video. In: Proceedings of the IEEE/CVF Conference on Computer Vision and Pattern Recognition. pp. 18995–19012 (2022)
37. Grauman, K., Westbury, A., Torresani, L., Kitani, K., Malik, J., Afouras, T., Ashutosh, K., Baiyya, V., Bansal, S., Boote, B., et al.: Ego-Exo4D: Understanding Skilled Human Activity from First- and Third-Person Perspectives. In: Proceedings of the IEEE/CVF Conference on Computer Vision and Pattern Recognition. pp. 19383–19400 (2024)
38. Guo, D., Wu, F., Zhu, F., Leng, F., Shi, G., Chen, H., Fan, H., Wang, J., Jiang, J., Wang, J., et al.: Seed1. 5-vl Technical Report. ArXiv Preprint ArXiv:2505.07062 (2025)
39. Guo, J., Rao, Z., Chen, Z., Zhou, J., Tao, D.: Fine-Grained Zero-Shot Learning: Advances, Challenges, and Prospects. ArXiv Preprint ArXiv:2401.17766 (2024)
40. Guo, L., Lu, Z., Yao, L.: Human-Machine Interaction Sensing Technology Based on Hand Gesture Recognition: A Review. IEEE Transactions on Human-Machine Systems **51**, 300–309 (2021)
41. Guo, L., Lu, Z., Yao, L.: Human-Machine Interaction Sensing Technology Based on Hand Gesture Recognition: A Review. IEEE Transactions on Human-Machine Systems **51**, 300–309 (2021)
42. Hashi, A.O., Hashim, S.Z.M., Asamah, A.B.: A Systematic Review of Hand Gesture Recognition: An Update From 2018 to 2024. IEEE Access **12**, 143599–143626 (2024)
43. He, K., Gkioxari, G., Dollár, P., Girshick, R.: Mask R-CNN. In: Proceedings of the IEEE International Conference on Computer Vision. pp. 2961–2969 (2017)
44. He, K., Zhang, X., Ren, S., Sun, J.: Deep Residual Learning for Image Recognition. In: Proceedings of the IEEE Conference on Computer Vision and Pattern Recognition. pp. 770–778 (2016)
45. Hong Da, N.L., Miura, J., Hayashi, K.: Enhancing Human-Robot Collaborative Search Through Efficient Space Sharing with On-Demand Bidirectional Interaction. In: European Conference on Computer Vision. pp. 20–35. Springer (2024)
46. Hu, R., Rohrbach, M., Andreas, J., Darrell, T., Saenko, K.: Modeling Relationships in Referential Expressions With Compositional Modular Networks. In: Proceedings of the IEEE Conference on Computer Vision and Pattern Recognition. pp. 1115–1124 (2017)
47. Huang, Z., Satoh, S.: LoA-Trans: Enhancing Visual Grounding by Location-Aware Transformers. In: European Conference on Computer Vision. pp. 405–421. Springer (2024)
48. Hummel, T., Karthik, S., Georgescu, M.I., Akata, Z.: EgoCVR: An Egocentric Benchmark for Fine-Grained Composed Video Retrieval. In: European Conference on Computer Vision. pp. 1–17. Springer (2024)
49. Hussain, M.: YOLO-v1 to YOLO-v8, the Rise of YOLO and Its Complementary Nature toward Digital Manufacturing and Industrial Defect Detection. Machines **11**, 677 (2023)
50. Ito, K., Kang, Y., Zhang, Y., Zhang, F., Biljecki, F.: Understanding Urban Perception with Visual Data: A Systematic Review. Cities **152**, 1–94 (2024)

51. Jiang, H., Lu, Z.: Visual Grounding for Object-Level Generalization in Reinforcement Learning. In: European Conference on Computer Vision. pp. 55–72. Springer (2024)
52. Jirak, D., Biertimpel, D., Kerzel, M., Wermter, S.: Solving Visual Object Ambiguities when Pointing: An Unsupervised Learning Approach. Neural Computing and Applications **33**(7), 2297–2319 (2021)
53. Ju, Y., Hu, K., Zhang, G., Zhang, G., Jiang, M., Xu, H.: Robo-ABC: Affordance Generalization Beyond Categories via Semantic Correspondence for Robot Manipulation. In: European Conference on Computer Vision. pp. 222–239. Springer (2024)
54. Kang, S., Kim, J., Kim, J., Hwang, S.J.: Your Large Vision-Language Model Only Needs A Few Attention Heads For Visual Grounding. In: Proceedings of the Computer Vision and Pattern Recognition Conference. pp. 9339–9350 (2025)
55. Kang, W., Liu, G., Shah, M., Yan, Y.: SegVG: Transferring Object Bounding Box to Segmentation for Visual Grounding. In: European Conference on Computer Vision. pp. 57–75. Springer (2024)
56. Kazemzadeh, S., Ordonez, V., Matten, M., Berg, T.: ReferItGame: Referring to Objects in Photographs of Natural Scenes. In: Proceedings of the 2014 Conference on Empirical Methods in Natural Language Processing. pp. 787–798 (2014)
57. Kusnanti, E.A., Sierra, E., Putra, G.G.S., Cahyadi, E.S., Haq, A., Purwitasari, D.: Indonesian Lexical Ambiguity in Machine Translation: A Literature Review. In: 2024 International Conference on Information Technology Research and Innovation (ICITRI). pp. 59–64. IEEE (2024)
58. Lee, J., Wang, J., Brown, E., Chu, L., Rodriguez, S.S., Froehlich, J.E.: GazePointAR: A context-aware multimodal voice assistant for pronoun disambiguation in wearable augmented reality. In: Proceedings of the 2024 CHI Conference on Human Factors in Computing Systems. pp. 1–20 (2024)
59. Li, Z., Xu, Q., Zhang, D., Song, H., Cai, Y., Qi, Q., Zhou, R., Pan, J., Li, Z., Tu, V., et al.: GroundingGPT: Language Enhanced Multi-modal Grounding Model. In: Proceedings of the 62nd Annual Meeting of the Association for Computational Linguistics. pp. 6657–6678 (2024)
60. Lin, T.Y., Maire, M., Belongie, S., Hays, J., Perona, P., Ramanan, D., Dollár, P., Zitnick, C.L.: Microsoft COCO: Common Objects in Context. In: Proceedings of the European Conference on Computer Vision. pp. 740–755 (2014)
61. Linderman, G.C., Rachh, M., Hoskins, J.G., Steinerberger, S., Kluger, Y.: Efficient Algorithms for t-distributed Stochastic Neighborhood Embedding. ArXiv Preprint ArXiv:1712.09005 (2017)
62. Liu, A., Feng, B., Xue, B., Wang, B., Wu, B., Lu, C., Zhao, C., Deng, C., Zhang, C., Ruan, C., et al.: DeepSeek-V3 Technical Report. ArXiv Preprint ArXiv:2412.19437 (2024)
63. Liu, C., Wei, H., Chen, J., Kong, L., Ge, Z., Zhu, Z., Zhao, L., Sun, J., Han, C., Zhang, X.: Focus Anywhere for Fine-grained Multi-page Document Understanding. ArXiv Preprint ArXiv:2405.14295 (2024)
64. Liu, H., Li, C., Li, Y., Lee, Y.J.: Improved baselines with visual instruction tuning. In: Proceedings of the IEEE/CVF conference on computer vision and pattern recognition. pp. 26296–26306 (2024)
65. Liu, J., Sun, W., Yang, H., Zeng, Z., Liu, C., Zheng, J., Liu, X., Rahmani, H., Sebe, N., Mian, A.: Deep Learning-Based Object Pose Estimation: A Comprehensive Survey. ArXiv Preprint ArXiv:2405.07801 (2024)

66. Liu, J., Chen, Q., Wang, Z., Tang, Y., Zhang, Y., Yan, C., Wang, D., Li, X., Zhao, B.: AerialVG: A Challenging Benchmark for Aerial Visual Grounding by Exploring Positional Relations. In: Proceedings of the IEEE/CVF International Conference on Computer Vision. pp. 5177–5187 (2025)
67. Liu, R., Liu, C., Bai, Y., Yuille, A.L.: CLEVR-Ref+: Diagnosing Visual Reasoning With Referring Expressions. In: Proceedings of the IEEE/CVF Conference on Computer Vision and Pattern Recognition. pp. 4185–4194 (2019)
68. Liu, S., Zeng, Z., Ren, T., Li, F., Zhang, H., Yang, J., Jiang, Q., Li, C., Yang, J., Su, H., et al.: Grounding DINO: Marrying DINO with Grounded Pre-training for Open-Set Object Detection. In: Proceedings of the European Conference on Computer Vision. pp. 38–55 (2024)
69. Liu, Y., Chen, W., Bai, Y., Liang, X., Li, G., Gao, W., Lin, L.: Aligning Cyber Space With Physical World: A Comprehensive Survey on Embodied AI. IEEE/ASME Transactions on Mechatronics pp. 1–22 (2025)
70. Ma'arif, A., Rahmaniar, W., Fathurrahman, H.I.K., Frisky, A.Z.K., et al.: Understanding of Convolutional Neural Network (CNN): A Review. International Journal of Robotics & Control Systems **2**(4) (2022)
71. Magay, A., Tripathi, D., Hao, Y., Fang, Y.: A Light and Smart Wearable Platform with Multimodal Foundation Model for Enhanced Spatial Reasoning in People with Blindness and Low Vision. In: European Conference on Computer Vision. pp. 323–339. Springer (2024)
72. Mao, J., Huang, J., Toshev, A., Camburu, O., Yuille, A.L., Murphy, K.: Generation and Comprehension of Unambiguous Object Descriptions. In: Proceedings of the IEEE Conference on Computer Vision and Pattern Recognition. pp. 11–20 (2016)
73. Memmi, M.Y., Slama, R., Berretti, S.: Hand Gesture Recognition Using Dual Graph Hierarchical Edges Representation and Graph Transformer Network. In: European Conference on Computer Vision. pp. 53–68. Springer (2024)
74. Mo, M., Wang, J., Wang, L., Chen, H., Gu, C., Leng, J., Gao, X.: NexusAD: Exploring the Nexus for Multimodal Perception and Comprehension of Corner Cases in Autonomous Driving. In: ECCV 2024 Workshop on Multimodal Perception and Comprehension of Corner Cases in Autonomous Driving (2024)
75. Nagaraja, V.K., Morariu, V.I., Davis, L.S.: Modeling Context between Objects for Referring Expression Understanding. In: Proceedings of the European Conference on Computer Vision. pp. 792–807 (2016)
76. Narasimhaswamy, S., Bhattacharya, U., Chen, X., Dasgupta, I., Mitra, S., Hoai, M.: HanDiffuser: Text-to-Image Generation With Realistic Hand Appearances. In: Proceedings of the IEEE/CVF Conference on Computer Vision and Pattern Recognition. pp. 2468–2479 (2024)
77. Oquab, M., Darcet, T., Moutakanni, T., Vo, H., Szafraniec, M., Khalidov, V., Fernandez, P., Haziza, D., Massa, F., El-Nouby, A., et al.: DINOv2: Learning Robust Visual Features without Supervision. ArXiv Preprint ArXiv:2304.07193 (2023)
78. Peng, Z., Wang, W., Dong, L., Hao, Y., Huang, S., Ma, S., Wei, F.: Kosmos-2: Grounding Multimodal Large Language Models to the World. ArXiv Preprint ArXiv:2306.14824 (2023)
79. Pepikj, B., Stark, M., Gehler, P., Schiele, B.: Occlusion Patterns for Object Class Detection. In: Proceedings of the IEEE Conference on Computer Vision and Pattern Recognition. pp. 3286–3293 (2013)
80. Pfeifer, R., Iida, F.: Embodied Artificial Intelligence: Trends and Challenges. Lecture Notes in Computer Science pp. 1–26 (2004)

81. Plummer, B.A., Wang, L., Cervantes, C.M., Caicedo, J.C., Hockenmaier, J., Lazebnik, S.: Flickr30k Entities: Collecting Region-to-Phrase Correspondences for Richer Image-to-Sentence Models. In: Proceedings of the IEEE International Conference on Computer Vision. pp. 2641–2649 (2015)
82. Pourpanah, F., Abdar, M., Luo, Y., Zhou, X., Wang, R., Lim, C.P., Wang, X.Z., Wu, Q.J.: A Review of Generalized Zero-Shot Learning Methods. IEEE Transactions on Pattern Analysis and Machine Intelligence **45**, 4051–4070 (2022)
83. Qi, Z., Dong, R., Zhang, S., Geng, H., Han, C., Ge, Z., Yi, L., Ma, K.: ShapeLLM: Universal 3D Object Understanding for Embodied Interaction. In: European Conference on Computer Vision. pp. 214–238. Springer (2024)
84. Qiao, Y., Deng, C., Wu, Q.: Referring Expression Comprehension: A Survey of Methods and Datasets. IEEE Transactions on Multimedia **23**, 4426–4440 (2020)
85. Radford, A., Kim, J.W., Hallacy, C., Ramesh, A., Goh, G., Agarwal, S., Sastry, G., Askell, A., Mishkin, P., Clark, J., et al.: Learning Transferable Visual Models From Natural Language Supervision. In: Proceedings of the International Conference on Machine Learning. pp. 8748–8763 (2021)
86. Schauerte, B., Fink, G.A.: Focusing Computational Visual Attention in Multi-Modal Human-Robot Interaction. In: Proceedings of the International Conference on Multimodal Interfaces and the Workshop on Machine Learning for Multimodal Interaction. pp. 1–8 (2010)
87. Schauerte, B., Richarz, J., Fink, G.A.: Saliency-Based Identification and Recognition of Pointed-At Objects. In: Proceedings of the IEEE/RSJ International Conference on Intelligent Robots and Systems. pp. 4638–4643 (2010)
88. Shi, C., Yang, S.: Spatial and Visual Perspective-Taking via View Rotation and Relation Reasoning for Embodied Reference Understanding. In: European Conference on Computer Vision. pp. 201–218. Springer (2022)
89. Shukla, D., Erkent, O., Piater, J.: Probabilistic Detection of Pointing Directions for Human-Robot Interaction. In: Proceedings of the 2015 International Conference on Digital Image Computing: Techniques and Applications. pp. 1–8 (2015)
90. Shukla, D., Erkent, Ö., Piater, J.: A Multi-View Hand Gesture RGB-D Dataset for Human-Robot Interaction Scenarios. In: Proceedings of the IEEE International Symposium on Robot and Human Interactive Communication. pp. 1084–1091 (2016)
91. Su, W., Miao, P., Dou, H., Li, X.: Scanformer: Referring Expression Comprehension by Iteratively Scanning. In: Proceedings of the IEEE/CVF Conference on Computer Vision and Pattern Recognition. pp. 13449–13458 (2024)
92. Team, G., Anil, R., Borgeaud, S., Alayrac, J.B., Yu, J., Soricut, R., Schalkwyk, J., Dai, A.M., Hauth, A., Millican, K., et al.: Gemini: A Family of Highly Capable Multimodal Models. arXiv preprint arXiv:2312.11805 (2023)
93. Team, G.R., Abeyruwan, S., Ainslie, J., Alayrac, J.B., Arenas, M.G., Armstrong, T., Balakrishna, A., Baruch, R., Bauza, M., Blokzijl, M., et al.: Gemini Robotics: Bringing AI into the Physical World. ArXiv Preprint ArXiv:2503.20020 (2025)
94. Touvron, H., Lavril, T., Izacard, G., Martinet, X., Lachaux, M.A., Lacroix, T., Rozière, B., Goyal, N., Hambro, E., Azhar, F., et al.: LLaMA: Open and Efficient Foundation Language Models. ArXiv Preprint ArXiv:2302.13971 (2023)
95. Vaswani, A., Shazeer, N., Parmar, N., Uszkoreit, J., Jones, L., Gomez, A.N., Kaiser, Ł., Polosukhin, I.: Attention is All you Need. In: Proceedings of the Advances in Neural Information Processing Systems. pp. 1–11 (2017)
96. Waisberg, E., Ong, J., Masalkhi, M., Zaman, N., Sarker, P., Lee, A.G., Tavakkoli, A.: Meta Smart Glasses—Large Language Models and the Future for Assistive Glasses for Individuals with Vision Impairments. Eye **38**, 1036–1038 (2024)

97. Wang, A., Liu, L., Chen, H., Lin, Z., Han, J., Ding, G.: YOLOE: Real-Time Seeing Anything. ArXiv Preprint ArXiv:2503.07465 (2025)
98. Wang, G., Xie, Y., Jiang, Y., Mandlekar, A., Xiao, C., Zhu, Y., Fan, L., Anandkumar, A.: Voyager: An Open-Ended Embodied Agent with Large Language Models. ArXiv Preprint ArXiv:2305.16291 (2023)
99. Wang, J., Shi, E., Hu, H., Ma, C., Liu, Y., Wang, X., Yao, Y., Liu, X., Ge, B., Zhang, S.: Large Language Models for Robotics: Opportunities, Challenges, and Perspectives. Journal of Automation and Intelligence **4**, 52–64 (2025)
100. Wang, P., Bai, S., Tan, S., Wang, S., Fan, Z., Bai, J., Chen, K., Liu, X., Wang, J., Ge, W., et al.: Qwen2-VL: Enhancing Vision-Language Model's Perception of the World at Any Resolution. ArXiv Preprint ArXiv:2409.12191 (2024)
101. Wang, W., Gao, Z., Gu, L., Pu, H., Cui, L., Wei, X., Liu, Z., Jing, L., Ye, S., Shao, J., et al.: InternVL3.5: Advancing Open-Source Multimodal Models in Versatility, Reasoning, and Efficiency. ArXiv Preprint ArXiv:2508.18265 (2025)
102. Watanabe, K.: Reflexive Attentional Shift Caused by Indexical Pointing Gesture. Journal of Vision **2**(7), 435–435 (2002)
103. Wu, Z., Chen, X., Pan, Z., Liu, X., Liu, W., Dai, D., Gao, H., Ma, Y., Wu, C., Wang, B., et al.: DeepSeek-VL2: Mixture-of-Experts Vision-Language Models for Advanced Multimodal Understanding. arXiv preprint arXiv:2412.10302 (2024)
104. Xian, Y., Schiele, B., Akata, Z.: Zero-Shot Learning - the Good, the Bad and the Ugly. In: Proceedings of the IEEE Conference on Computer Vision and Pattern Recognition. pp. 4582–4591 (2017)
105. Xiao, B., Wu, H., Xu, W., Dai, X., Hu, H., Lu, Y., Zeng, M., Liu, C., Yuan, L.: Florence-2: Advancing a Unified Representation for a Variety of Vision Tasks. In: Proceedings of the IEEE/CVF Conference on Computer Vision and Pattern Recognition. pp. 4818–4829 (2024)
106. Xiao, L., Yang, X., Lan, X., Wang, Y., Xu, C.: Towards Visual Grounding: A Survey. ArXiv Preprint ArXiv:2412.20206 (2024)
107. Xiao, L., Yang, X., Lan, X., Wang, Y., Xu, C.: Towards Visual Grounding: A Survey. IEEE Transactions on Pattern Analysis and Machine Intelligence (2025)
108. Xiao, L., Yang, X., Peng, F., Wang, Y., Xu, C.: OneRef: Unified One-tower Expression Grounding and Segmentation with Mask Referring Modeling. In: Proceedings of the Advances in Neural Information Processing Systems. pp. 139854–139885 (2024)
109. Xie, P., Chen, S., Dai, Y., Hu, D., Yang, K., Wang, G.: Target-Oriented Object Grasping via Multimodal Human Guidance. In: European Conference on Computer Vision. pp. 305–322. Springer (2024)
110. Yang, A., Li, A., Yang, B., Zhang, B., Hui, B., Zheng, B., Yu, B., Gao, C., Huang, C., Lv, C., et al.: Qwen3 Technical Report. ArXiv Preprint ArXiv:2505.09388 (2025)
111. Yang, J., Ding, R., Brown, E., Qi, X., Xie, S.: V-IRL: Grounding Virtual Intelligence in Real Life. In: European conference on computer vision. pp. 36–55. Springer (2024)
112. Yang, S., Li, G., Yu, Y.: Dynamic Graph Attention for Referring Expression Comprehension. In: Proceedings of the IEEE/CVF International Conference on Computer Vision. pp. 4644–4653 (2019)
113. You, H., Zhang, H., Gan, Z., Du, X., Zhang, B., Wang, Z., Cao, L., Chang, S.F., Yang, Y.: Ferret: Refer and Ground Anything Anywhere at Any Granularity. ArXiv Preprint ArXiv:2310.07704 (2023)

114. Yu, L., Lin, Z., Shen, X., Yang, J., Lu, X., Bansal, M., Berg, T.L.: MAttNet: Modular Attention Network for Referring Expression Comprehension. In: Proceedings of the IEEE Conference on Computer Vision and Pattern Recognition. pp. 1307–1315 (2018)
115. Yu, L., Poirson, P., Yang, S., Berg, A.C., Berg, T.L.: Modeling Context in Referring Expressions. In: Proceedings of the European Conference on Computer Vision. pp. 69–85 (2016)
116. Zhang, H., Niu, Y., Chang, S.F.: Grounding Referring Expressions in Images by Variational Context. In: Proceedings of the IEEE Conference on Computer Vision and Pattern Recognition. pp. 4158–4166 (2018)
117. Zhang, H., Li, F., Liu, S., Zhang, L., Su, H., Zhu, J., Ni, L.M., Shum, H.Y.: DINO: DETR with Improved DeNoising Anchor Boxes for End-to-End Object Detection. ArXiv Preprint ArXiv:2203.03605 (2022)
118. Zhang, H., Li, H., Li, F., Ren, T., Zou, X., Liu, S., Huang, S., Gao, J., Leizhang, Li, C., et al.: LLaVA-Grounding: Grounded Visual Chat with Large Multimodal Models. In: Proceedings of the European Conference on Computer Vision. pp. 19–35 (2024)
119. Zhao, Y., Jiang, J., Chen, Y., Liu, R., Yang, Y., Xue, X., Chen, S.: Metaverse: Perspectives from Graphics, Interactions and Visualization. Visual Informatics **6**, 56–67 (2022)
120. Zhuang, B., Wu, Q., Shen, C., Reid, I., Van Den Hengel, A.: Parallel Attention: A Unified Framework for Visual Object Discovery Through Dialogs and Queries. In: Proceedings of the IEEE Conference on Computer Vision and Pattern Recognition. pp. 4252–4261 (2018)

6 Supplementary Material

Related Work

Perception from an egocentric perspective is crucial in Embodied AI [28, 69, 80, 98], robotics [11, 35, 93, 99], and Augmented Reality (AR) [7, 13]. In egocentric interactions [10, 36, 37], the hand plays a key role not only in actions but also in communication and pointing [15, 87]. Pointing gestures are critical for providing spatial grounding for language [42, 76]. Prior work on hand-object interactions [10, 36, 37] and datasets like YouRefit Pointing at Objects [18] have explored pointing gestures, while others like referAT [86] and PointAt [87] integrate language for object reference tasks. However, these datasets either focus on long-term actions (e.g., "cooking") without fine-grained instantaneous reference annotations or offer limited interaction cues [41, 42, 119]. Our dataset focuses on a key moment: an instant where an object is referenced by a hand gesture in the first-person view. True embodied interaction requires models to understand not just "what is happening," but "what is being referenced."

6.1 Visual Grounding

Visual Grounding [4, 24, 106, 108, 116, 120], particularly Referring Expression Comprehension (REC) [46, 84, 91, 112, 114], aims to localize the region in an image corresponding to a natural language description.

Traditional REC and Viewpoint Limitations Traditional REC tasks have been extensively studied under the third-person viewpoint. Classic datasets, such as RefCOCO [60, 115], RefCOCO+ [72], and RefCOCOg [75], have driven the evolution of models from CNN-based [20, 43, 44, 49, 70, 97] architectures to Transformers [91, 95]. Recently, open-vocabulary detectors like Grounding DINO [68, 77, 117] and YOLO-World [20, 49, 97] have demonstrated strong performance on these benchmarks. However, these datasets and models represent a limited definition of visual perception [29, 50]. They primarily stem from isolated captures in a "bystander" view, completely neglecting the presence of an interacting agent (e.g., a user), let alone non-verbal cues such as hand gestures and intentions.

Towards Egocentric Visual Grounding Migrating the REC task to the egocentric viewpoint introduces unique challenges, such as severe object occlusion [14, 79], drastic viewpoint changes [29, 50], and visual interference caused by the hand itself [5, 65, 76]. Crucially, the hand also offers a key piece of structured non-verbal information. Distinct from prior research, our work explicitly treats the hand gesture as a signal, rather than noise, aiming to study the complex, tripartite relationship between language, gesture, and the visual target.

6.2 MLLMs for REC

In recent years, Multimodal Large Language Models (MLLMs) [1, 22, 62, 92, 94, 118], such as LLaVA [118], Ferret [113], Qwen-VL [8, 110], and kosmos [78], have significantly enhanced visual understanding and localization generalization, including zero-shot [9, 82, 104] capabilities, through pre-training on vast image-text data. Models like Ferret [113] have demonstrated the potential to output bounding boxes directly, addressing the REC task. Nevertheless, their core framework remains primarily centered on (image, text) alignment. They lack an effective mechanism to integrate fine-grained [21, 39, 63], structured non-verbal information, such as the 2D pose of a pointing gesture or precise physical spatial relationships [5, 65].

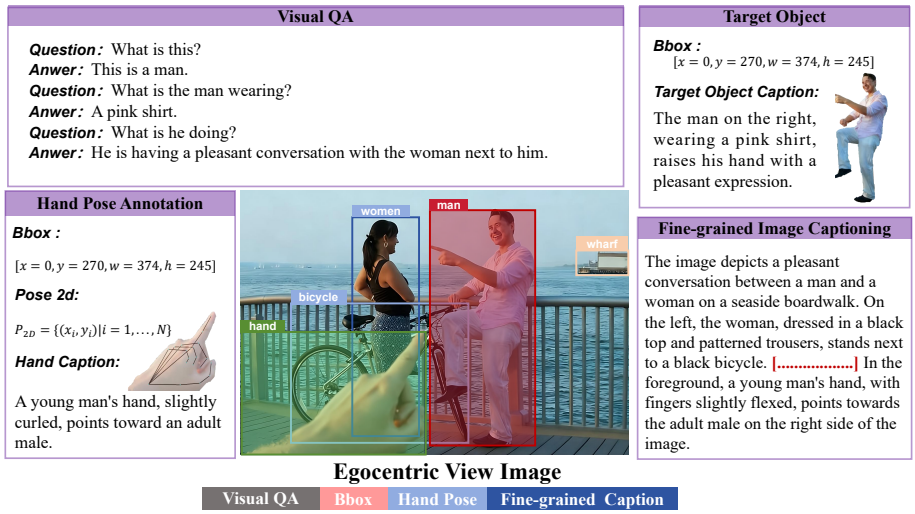

Fig. 7: Overview of the Egopoint-ground Dataset and its Core Annotations. The Egopoint-ground dataset comprises first-person-perspective images captured via smart glasses, depicting a hand pointing towards a target object. The dataset features four primary annotations for each image: 1) Target Object Annotation: Includes the object's bounding box, textual description, and essential attributes. 2) Fine-grained Description: Detailed linguistic descriptions of the overall scene and the deictic (referential) interaction. 3) High-Quality Visual QA Pairs: Question-and-answer pairs focusing on the target object and the interaction intent. 4) First-Person Hand Pose and Action: Provides the hand's bounding box, 2D keypoint pose, and precise action description, serving as a key non-verbal spatial anchor.

7 Dataset Statistics and Composition

Our dataset is designed to cover complex human-computer interaction scenarios from a First-Person View. The dataset comprises several dozen independent scenarios, encompassing hundreds of different object and action categories.

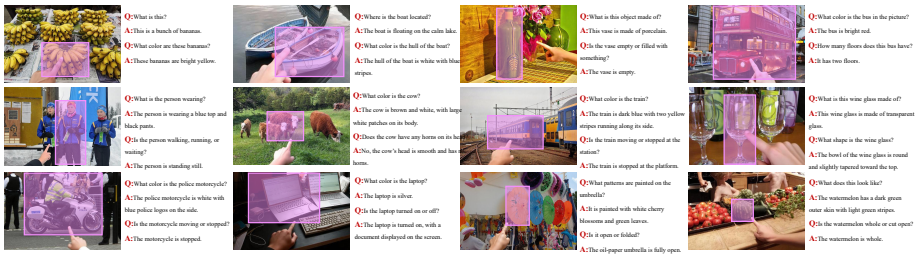

Fig. 8: Example of the Visual Question Answering Section for Object Pointing, Showcased via Random Sampling.

Fig. 9: Display of Randomly Sampled Image Captions.

The data sources are divided into three parts, as shown in Table 5.

The dataset mainly includes: home scenarios, campus scenarios, daily interaction scenarios, supermarket/mall interaction scenarios, and others. For the detailed categories and corresponding IDs of the dataset, please refer to Appendix Table 10.

To provide a comprehensive view of the dataset's features, we have augmented the data presentation with detailed examples. Figure 7 offers a representative showcase of the dataset's augmented data. Specifically, Figure 8 illustrates Visual Question Answering (VQA) examples for the pointed target objects, while Figure 9 presents image captioning examples for the entire scene.

7.1 Data Annotation Methodology

The dataset annotation adopts a hybrid model combining manual fine-grained annotation with algorithmic pre-annotation. The annotators are mainly researchers from various universities who possess rich expertise in computer vision. Among the annotators, males account for 75%, and females account for 25%.

Table 5: Data Source Composition

Source	Ratio
Real-World Data	39.35%
Synthetic Generation	38.96%
Image Editing	21.69%

7.2 Data Acquisition Details

The manual collection part of the dataset primarily utilizes RayNeo smart glasses (Model: RayNeo V3). The key parameters of this device are as shown in Table 6.

Table 6: Key Parameters of RayNeo V3

Parameter	Specification
Model	RayNeo V3
Sensor	Sony IMX681, 12MP
Lens	5P customized F2.2 large aperture 16mm ultra-wide-angle
Algorithm	ArcSoft customized algorithm
ISP	1st generation Snapdragon AR1 dual ISP

Table 7: Model Specifications and Evaluation Metrics. (Test on Egocentric Deictic Visual Grounding - EDG)

Model Name	Model Size	Inference Time (h:min)	Peak VRAM Usage	Model Source
Qwen3-VL-8B	8.78 B	1:47	16.6 GB	Open-Sourced Model
Florence-2-large	0.77 B	0:36	1.8 GB	Open-Sourced Model
Ferret	13.37 B	4:52	26.9 GB	Open-Sourced Model
LLaVA-OneVision-1.5-8B-Instruct	8.53 B	1:58	16.3 GB	Open-Sourced Model
GroundingGPT	7.90 B	1:52	16.5 GB	Open-Sourced Model
InternVL-3.5-8B	7.91 B	2:21	40.2 GB	Open-Sourced Model

All collected data has undergone privacy protection processing. Areas involving facial or Personally Identifiable Information (PII) have been blurred to ensure compliance with data ethics requirements.

8 Experiment Details

We have organized the code for our method in the `codes` directory. Upon publication, we will release the code and pretrained models. Detailed usage instructions are provided in `/codes/EgoPoint-Ground_code/README.md`.

8.1 Experimental Settings

All experiments are conducted with the official task scripts in `code_for_evaluate_on_Ego` under inference-only settings (no task-specific fine-tuning). Across REC/POG/EDG/D-VQA, each script loads model checkpoints via `from_pretrained(..., device_map="auto")` and runs mixed-precision inference (typically `bf16` in the provided `run.sh` files). The arguments `-start/-end` are used to control the evaluated sample range (`end=-1` indicates the full split).

For REC and EDG, the target instance is sampled from the non-hand annotations; each sample is evaluated over its `underspecified_referent` entries (typically three expressions), and each expression is treated as an independent test case. For POG and EDG, the hand box is taken from `ann_id=anno_hand`, and the GT pointed object is selected from non-hand annotations. For D-VQA, the hand box is also taken from `ann_id=anno_hand`, and the GT category is extracted from `category_name` in non-hand annotations.

Prompt templates are task-specific but parser-aligned: REC uses underspecified text only, POG uses hand bbox only, EDG uses both hand bbox and underspecified text, and D-VQA uses hand bbox with a question (e.g., "what is this?") to prompt category prediction of the pointed object. Coordinate formats are adapted per model/script (`absolute`, `relative_1`, or `relative_1000`), then converted to a unified absolute box space for scoring. Most scripts use deterministic decoding (`do_sample=False`); model-specific official settings are preserved where required (e.g., sampling-based decoding in some GroundingGPT/DeepSeek-VL2 scripts). All scripts enforce short final bbox outputs (instead of long reasoning traces) to ensure stable parsing and fair comparison.

8.2 Other Details in Experiments

To support reproducibility, each evaluation JSON includes both run metadata and per-sample records. Metadata contains model path, data path, coordinate mode, sample count, parsed prediction count (`parsed_ok`), valid IoU count, and skip/error statistics (e.g., `missing_target`, `missing_hand_bbox`, `parse_failed`, `infer_exception`). Per-sample entries store GT/predicted boxes in both absolute and relative formats (when available), raw model outputs, and error tags.

Box extraction is implemented with a JSON-first parser (e.g., `{"bbox_2d": [x1, y1, x2, y2]}`) plus regex fallback for list-form outputs. Predicted and GT boxes are sanitized, clamped to image boundaries, and converted across coordinate systems before metric computation. Metrics are uniformly reported as `IoU@0.3`, `IoU@0.5`, `IoU@0.7`, and `IoU_avg`. In addition, scripts save qualitative diagnostics in `visualize/<model_name>/`, including overlay images (GT/pred/hand when applicable) and paired prompt/raw-output text files, which support error analysis and result verification.

To comprehensively evaluate the performance of general-purpose models on our dataset, we summarize key efficiency metrics for each baseline, including inference latency, peak VRAM consumption, and model parameter count, as presented in Table 7. Furthermore, to ensure experimental fairness and reproducibility, we detail the specific input paradigms employed for each model across the D-REC and POG tasks in Tables 8 and Table 9, respectively.

Table 8: Model Input Paradigms (Test on Language-Only Grounding (D-REC))

Model Name	**Input Paradigm**
GroundingGPT	"[object caption]"
Qwen3-VL	"You are given an egocentric (first-person) image where a visible hand/finger is pointing to an object. Your task is to localize the pointed-at target object and output its bounding box. Use [x1, y1, x2, y2] coordinates in range [0, 1000] (relative to image size). The underspecified reference below is auxiliary text about the target. Underspecified reference: {underspecified_referent}. Return ONLY one JSON object in this format: {"bbox_2d": [x1, y1, x2, y2]}."
InternVL-3.5	"You are given an egocentric (first-person) image where a visible hand/finger is pointing to an object, predict the bounding box of <ref>{underspecified_referent}</ref> being pointed at in format [x1, y1, x2, y2] where coordinates are in range [0, 1000] (relative to image size). Return ONLY the bbox of the pointed object in format [x1, y1, x2, y2]. Give me the result directly, do not reason."
LLaVA-OneVision	"You are given an egocentric (first-person) image where a visible hand/finger is pointing to an object. Your task is to localize the pointed-at target object and output its bounding box, where each coordinate is normalized to [0, 1] relative to image width/height. Underspecified reference: {underspecified_referent}. Return ONLY the bbox in this exact format: [x1, y1, x2, y2]."
Ferret	"You are given an egocentric (first-person) image where a visible hand/finger is pointing to an object. Your task is to localize the pointed-at target object and output its bounding box in format [x1, y1, x2, y2], where coordinates are in range [0, 1000] (relative to image size). Underspecified reference: {underspecified_referent}. Return ONLY the bbox of the pointed object as [x1, y1, x2, y2]."
DeepSeek-VL2	"<|grounding|> You are given an egocentric (first-person) image where a visible hand/finger is pointing to an object. Your task is to localize the pointed-at target object and output its bounding box in format [x1, y1, x2, y2], where each coordinate is in [0, 1000] relative to image size. Target object's underspecified reference: {underspecified_referent}. Return ONLY one bbox in [x1, y1, x2, y2]."

Table 9: Model Input Paradigms (Test on Pointing Only Grounding - POG)

Model Name	**Input Paradigm**
GroundingGPT	"You are a pointed object bounding box detector. Given an image and a hand bbox, predict the bounding box of the object being pointed at in format [x1, y1, x2, y2]. Hand bbox (xyxy, normalized to [0,1]): {hand_input}. Return ONLY the bbox of the pointed object in this format: [x1, y1, x2, y2]."
Qwen3-VL	"You are a pointed object bounding box detector. Given an image and a hand bbox, predict the bounding box of the object being pointed at in format [x1, y1, x2, y2] where coordinates are in range [0, 1000] (relative to image size). Input hand bbox: {hand_input}. Return ONLY the bbox of the hand-pointed object in this format: {"bbox_2d": [x1, y1, x2, y2]}."
InternVL-3.5	"You are a pointed object bounding box detector. Given an image and a hand bbox, predict the bounding box of <ref>the object being pointed</ref> in format [x1, y1, x2, y2] where coordinates are in range [0, 1000] (relative to image size). Input hand bbox: {hand_input}. Return ONLY the bbox of the pointed object in format [x1, y1, x2, y2]."
LLaVA-OneVision	"You are a pointed object bounding box detector. Given an image and a hand bbox, predict the bounding box of the object being pointed at in format [x1, y1, x2, y2], where each coordinate is normalized to [0, 1] relative to image width/height. Input hand bbox (xyxy, normalized to [0, 1]): {hand_input}. Return ONLY the bbox in this exact JSON format: [x1, y1, x2, y2]."
Ferret	"You are a pointed object bounding box detector. Given an image and a hand bbox, predict the bounding box of the object being pointed at in format [x1, y1, x2, y2] where coordinates are in range [0, 1000] (relative to image size). Input hand bbox: {hand_input}. Return ONLY about the POINTED OBJECT, do not mention the hand, do not reason, return the result directly as [x1, y1, x2, y2]."
DeepSeek-VL2	"<|grounding|> You are a pointed object grounding model. Given an image and a hand bbox, predict the bbox of the object being pointed at in format [x1, y1, x2, y2] where coordinates are in [0, 1000] relative to image size. Input hand bbox: {hand_input}. Return ONLY one bbox in [x1, y1, x2, y2]."

Table 10: Detailed Mapping of Dataset Object Categories to Their Corresponding Integer IDs.

Category	ID	Category	ID	Category	ID	Category	ID	Category	ID	Category	ID
advertising board	0	airplane	1	alarm	2	ammeter	3	apple	4	artwork	5
ashtray	6	audio equipment	7	axe	8	backpack	9	bag	10	ball	11
ball of thread	12	ballpoint pen	13	banana	14	band-aid	15	baseball bat	16	basketball	17
bear	18	bed	19	beer	20	bell	21	belt	22	bench	23
beverage	24	bicycle	25	bike	26	bird	27	blackboard	29	blanket	30
board	31	boat	32	book	33	bookshelf	34	bottle	35	bouquet of flowers	36
bowl	37	box	38	bread	39	broccoli	40	brush	41	bucket	42
bus	43	bus stop	44	button	45	cabinet	46	cake	47	calculator	48
calendar	49	camera	50	can	51	candy	52	car	53	card	54
carrot	55	castle	56	cat	57	cattle	58	cd	59	cell phone	60
chain	61	chair	62	chandelier	63	charger	64	chicken	65	chocolate	66
church	67	circuit board	68	cling film	69	clock	70	cloth	71	clothes	72
coat	73	coffee	74	coffee machine	75	coin	76	corn	77	cosmetics	78
cotton swab	79	couch	80	cow	81	crane	82	cup	83	curtain	84
dining table	85	disc	87	dog	88	doll	89	donut	90	door	91
door handle	92	duck	93	dumbbell	94	ear stud	95	egg	96	electric drill	97
elephant	98	elevator	99	eye drops	100	fan	101	fence	102	file	103
fire engine	104	fire extinguisher	105	fire hydrant	106	fireplace	107	fireworks	108	fish	109
fishhook	110	fishing hook	111	fishing line	112	fishing rod	113	fitness equipment	114	flag	115
flashlight	116	flour	117	flower	118	flowerpot	119	folding chair	120	food	121
fork	122	fragrance device	123	fries	124	frisbee	125	galvanometer	126	game boy	127
game console	128	game controller	129	game disc	130	giraffe	131	glasses	132	globe	133
gloves	134	goat	135	goblet	136	golf club	137	grape	138	green onion	139
guitar	140	hair drier	141	hair dryer	142	hamburger	143	hand	144	handbag	145
hat	146	head	147	headphones	148	helmet	149	highball glass	150	hole	151
hook	152	horse	153	hot dog	154	hula hoop	155	iron hammer	156	jam	157
jeans	158	jewelry	159	juice	160	juicer	161	kettle	162	key	163
keyboard	164	kid	165	kite	166	knee pads	167	knife	168	lamp	169
laptop	170	leaf	171	led lamp	172	lemon	173	lens cap	174	light bulb	175
lighthouse	176	lipstick	177	lock	178	lubricating oil	179	machine	180	magazine	181
mailbox	182	meat	183	medicine	184	microwave	185	milk	186	mirror	187
model	188	monitor	189	monument	190	motorcycle	191	mouse	192	nail	193
nail art sheet	194	necklace	195	needle	196	net	197	newspaper	198	notebook	199
nut	200	orange	202	oven	203	overcoat	204	painting	205	pan	206
paper	207	paper bag	208	parking meter	209	pen	211	pen holder	212	pencil	213
pepper powder	215	person	216	phone	217	phone booth	218	photo	219	piano	220
pigment	221	pigment tray	222	pillar	223	pillow	224	pizza	225	pizza box	226
plant	227	plate	228	pliers	229	porcelain	230	pot	231	potted plant	232
rack	233	radio	234	reagent bottle	235	red-crowned crane	236	refrigerator	237	remote	238
rice	239	rice cooker	240	road sign	241	rockery	242	rose	243	sachs	244
salt	245	sandals	246	sandwich	247	sausage	248	saw	249	scale	250
scarf	251	scissors	252	screw	253	screwdriver	254	sculpture	255	seasoning	256
shampoo	257	sheep	258	shoes	259	shop	260	shopping cart	261	showerhead	262
signboard	263	signpost	264	sink	265	skateboard	266	skis	267	slippers	268
snack	269	snowboard	270	soap	271	socket	272	sofa	273	soup	274
soy sauce	275	spoon	276	sports ball	277	squirrel	278	stapler	279	star	280
stick	281	sticker	282	sticky note	283	stirring rod	284	stone	285	strawberry	287
string	288	suitcase	289	sunflower	290	sunglasses	291	surfboard	292	t-shirt	293
table	294	tape measure	295	teddy bear	296	tennis racket	297	test tube	298	tie	299
timer	300	tire	301	toaster	302	toilet	303	tomato	304	tools	305
toothbrush	306	toothpaste	307	towel rack	308	toy	309	toy house	310	trachea	311
track	312	traffic light	313	train	314	transformer	315	tree	316	trousers	317
truck	318	trunk	319	tv	320	umbrella	321	usb flash drive	322	vase	323
vending machine	325	violin	326	vitamin	327	vr glasses	328	wall	329	wallet	330
water	331	watering pot	332	watermelon	333	whiteboard	334	window	335	wine	336
wine bottle	337	wine glass	338	wire	339	wooden block	340	wooden board	341	wool ball	342
wrench	343	yoga wheel	344	zebra	345	hot water bottle	346	ruler	347	chopsticks	348
chopstick	349	conditioner	350								